

Hints of tensions in the cosmic microwave background temperature and polarization quadrupoles

Jahmour J. Givans^{1,2,*} and Marc Kamionkowski³

¹*Center for Computational Astrophysics, Flatiron Institute, 162 5th Ave, New York, NY 10010, USA*

²*Department of Astrophysical Sciences, Peyton Hall,
Princeton University, Princeton, NJ 08544, USA*

³*William H. Miller III Department of Physics & Astronomy,
Johns Hopkins University, 3400 N. Charles St., Baltimore, MD 21218, USA*

(Dated: November 13, 2023)

The large-angular-scale falloff in the autocorrelation function for the cosmic microwave background (CMB) temperature has long intrigued cosmologists and fueled speculation about suppressed superhorizon power. Here we highlight an inconsistency between the temperature quadrupole and the more recently obtained E-mode polarization quadrupole from Planck PR3. The temperature quadrupole arises primarily at the CMB surface of last scatter, while the polarization primarily from the epoch of reionization, but the two still probe comparable distance scales. Although the temperature quadrupole is intriguingly low (much greater than a 1σ fluctuation) compared with that expected in the standard Λ CDM cosmological model, the polarization quadrupole turns out to be somewhat high, at the 1σ level. We calculate the joint probability distribution function for both and find a slight tension: the observed pair of quadrupoles is inconsistent at a 2.3σ confidence level. The problem is robust to simple changes to the cosmological model. If the high polarization quadrupole survives further scrutiny, then this result disfavors, at comparable significance, new superhorizon physics. The full-sky coverage and pristine foreground subtraction of the LiteBIRD satellite will be ideal to help resolve this question.

I. INTRODUCTION

The dropoff in the cosmic microwave background (CMB) temperature autocorrelation function at the largest angular scales has intrigued cosmologists ever since it was first seen in the Cosmic Background Explorer (COBE) Differential Microwave Radiometer (DMR) maps [1]. This dropoff is seen in the correlation function at angular separations $\Delta\theta \gtrsim 60^\circ$. In harmonic space, it is manifest as an unusually low temperature quadrupole (C_2) [1–3]; it is about one fifth the value expected from extrapolation of the power spectrum (C_l) at higher multipoles l .

This fluctuation is nothing to lose sleep over, especially if you take into account the look-elsewhere effect (of the thousands of multipole moments that have been measured, you’d expect a few to stray from the curve). But on the other hand, the quadrupole probes the largest observationally accessible distance scales in the Universe. Maybe there’s something happening at larger, superhorizon, distances, and this is just the tip of the iceberg? This possibility has fueled a number of ideas for new superhorizon physics [4–16], and motivates the search for other ways to access information on these superhorizon scales.

One avenue of investigation [17–20] has involved study of the statistical significance of the dearth of large-angle correlations, the possibility of cross-correlations between different multipole moments that affect the interpretation. The conclusion, though, is that cosmic variance,

the sample variance that arises from the finite number of $\sim 60^\circ$ patches on the sky, prevents the statistical significance to rise much beyond the $\sim 2\sigma$ level. Another avenue, though, is to seek other observables that probe the largest distance scales and that may thus provide complementary information. Ideas along these lines include the additional information provided by lensing maps [21] and large-scale polarization fluctuations in the CMB [22, 23]. The latter was considered by the Planck Collaboration in two different ways: Ref. [20] generalized the analysis of the temperature autocorrelation function to include temperature-polarization cross-correlation and polarization autocorrelations—the conclusions of prior work were essentially unchanged. Ref. [24] took all the polarization and temperature information to test the possibility that the cosmic curvature power spectrum might be suppressed at superhorizon scales. Even with polarization, cosmic variance limits what can be said: the data do not call for a suppression of power.

Our purpose here is to highlight and discuss the implications of a related curious feature in the large-angle CMB polarization, as seen in the leftmost side of Figs. 1 and 2 in Ref. [3], which show, respectively, the CMB temperature and polarization power spectra (and also the temperature-polarization cross-correlation). The first Figure shows the longstanding low CMB temperature quadrupole, the feature that has led over the past thirty years to the speculation that something interesting may be happening at superhorizon scales. The second Figure, however, shows something surprising: The *polarization* quadrupole is *high*. The occurrence of a low temperature quadrupole and a high polarization quadrupole warrants attention. It is noteworthy because none of the other

* Email: jgivans@flatironinstitute.org

lowest multipole moments show such a discrepancy and even moreso if viewed as our best portal to superhorizon physics.

We quantify the discrepancy by calculating the joint probability distribution function (PDF) for the two quadrupoles and estimate that they are inconsistent at a 2.3σ level, a conclusion robust to changes in the cosmological model. Given that the temperature quadrupole has now been obtained independently by three different satellite missions, we surmise that there may be issues with instrumental systematics and/or foreground removal in Planck. If not, though, it suggests that new-physics explanations for the low temperature quadrupole are disfavored. The discrepancy highlights the importance of LiteBIRD's improved measurements of these quadrupoles [25].

This paper is organized as follows: in Sections II and III we review the statistics of CMB multipole coefficients and their power spectra under the assumptions of Λ CDM cosmology, or more generally, a cosmological model with perturbations that are statistically isotropic/homogeneous and Gaussian.¹ In Section IV we quantify the discrepancy between the temperature and polarization quadrupoles and their Λ CDM predictions; we show that the magnitude of this discrepancy grows when considering their joint probability. Superhorizon modifications to Λ CDM which would shift the quadrupole values are explored in Section V. We summarize our findings with a view toward LiteBIRD in Section VI.

II. CMB MULTIPOLES AND POWER SPECTRA

The standard Λ CDM cosmological model tells us that inflation produced adiabatic, nearly scale-invariant, and Gaussian primordial scalar (i.e. curvature) perturbations; these perturbations are the seeds that later induce CMB temperature and E-mode polarization anisotropies. The observed anisotropy patterns may be expanded in terms of spherical harmonics. For temperature anisotropies this takes the form,

$$T(\mathbf{n}) = \sum_{l=1}^{\infty} \sum_{m=-l}^l a_{lm}^T Y_{lm}(\mathbf{n}), \quad (1)$$

which can be inverted to give harmonic coefficients,

$$a_{lm}^T = \int d^2\mathbf{n} T(\mathbf{n}) Y_{lm}^*(\mathbf{n}). \quad (2)$$

¹ A recent paper exploring the joint probability of four different CMB anomalies occurring together has called into question the assumption of statistical isotropy [26]. Our paper does not address this consideration.

In the case of polarization anisotropies, we first decompose the sky pattern using Stokes Q and U parameters to get

$$(Q \pm iU)(\mathbf{n}) = \sum_{l=1}^{\infty} \sum_{m=-l}^l a_{lm}^{(\pm 2)} Y_{lm}(\mathbf{n}), \quad (3)$$

where $Y_{lm}(\mathbf{n})$ are the spin-2 spherical harmonic functions which are required since polarization is a spin-2 quantity. The associated harmonic coefficients are

$$a_{lm}^{(\pm 2)} = \int d^2\mathbf{n} (Q \pm iU)(\mathbf{n}) Y_{lm}^*(\mathbf{n}), \quad (4)$$

which can easily be converted to E-mode coefficients

$$a_{lm}^E = -\frac{1}{2} \left(a_{lm}^{(+2)} + a_{lm}^{(-2)} \right). \quad (5)$$

Each a_{lm} is drawn from a Gaussian with zero mean but nonzero variance—or angular power spectrum— C_l given by,

$$\langle a_{lm}^X a_{l'm'}^{Y*} \rangle = \delta_{ll'} \delta_{mm'} C_l^{XY}, \quad (6)$$

where $X, Y \in \{T, E\}$.

III. THE ORIGINS OF THE QUADRUPOLES

While both types of CMB anisotropies trace their origins to primordial curvature perturbations, the timescales over which their respective power spectra receive their greatest contributions differ. From a distribution of primordial curvature perturbations $\zeta(\mathbf{k})$ with power spectrum defined via

$$\langle \zeta(\mathbf{k}) \zeta^*(\mathbf{k}') \rangle = P_\zeta(k) \delta(\mathbf{k} - \mathbf{k}'), \quad (7)$$

and dimensionless power spectrum $\mathcal{P}_\zeta(k) = k^3 P_\zeta(k) / 2\pi^2$, one can calculate the CMB angular power spectra,

$$C_l^{XY} = 4\pi \int \frac{dk}{k} \mathcal{P}_\zeta(k) \Delta_l^X(k, \eta_0) \Delta_l^Y(k, \eta_0), \quad (8)$$

where $\Delta_l^X(k, \eta_0)$ are the photon transfer functions evaluated today. These can be obtained numerically, e.g., from a Boltzmann code like CLASS [27] or CAMB [28]. For the quadrupole, the E-mode transfer function can be approximated by [29]

$$\Delta_2^E(k, \eta_0) \simeq -\frac{2\sqrt{6}}{3} \int_0^{\eta_0} d\eta g(\eta) \frac{j_2[k(\eta_0 - \eta)]}{[k(\eta_0 - \eta)]^2} j_2[k(\eta - \eta_*)], \quad (9)$$

where η_0 is the conformal time today and η_* that at recombination, and $g(\eta)$ is the visibility function for reionization; it integrates to the reionization optical depth

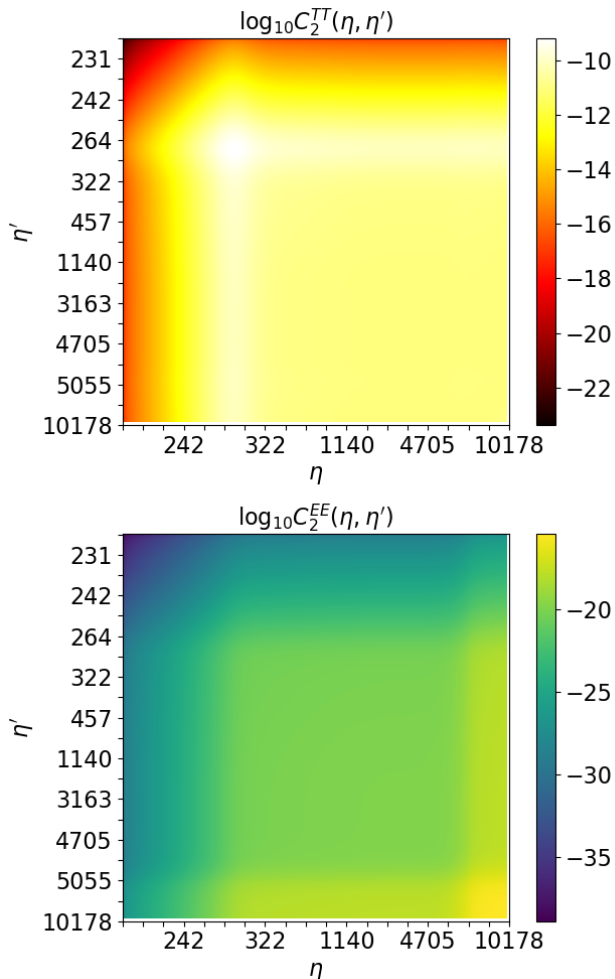


FIG. 1. Logarithm of the conformal-time integrands of the temperature (top) and E-mode polarization (bottom) quadrupoles.

$\tau = \int d\eta g(\eta)$ and peaks at the conformal time of reionization. The temperature transfer function can be approximated by

$$\Delta_2^T(k, \eta_0) \simeq -\frac{2}{9} j_2[k(\eta_0 - \eta_*)]. \quad (10)$$

It is determined primarily by the quadrupole at the surface of last scatter and has an $O(\tau)$ correction (not shown) from reionization and also a small contribution from the integrated Sachs-Wolfe effect. Fig. 1 shows contributions to the CMB TT (top) and EE (bottom) power spectra as functions of η and η' , using exact results from CLASS [27].

Even though the peaks of recombination and reionization transfer functions occur at substantially different redshifts ($z_* \sim 1100$ and $z_{re} \sim 6$, respectively), the comoving distances to their surfaces are comparable. Consequently, the two probe a comparable range of physical separations, as shown in Fig. 2.

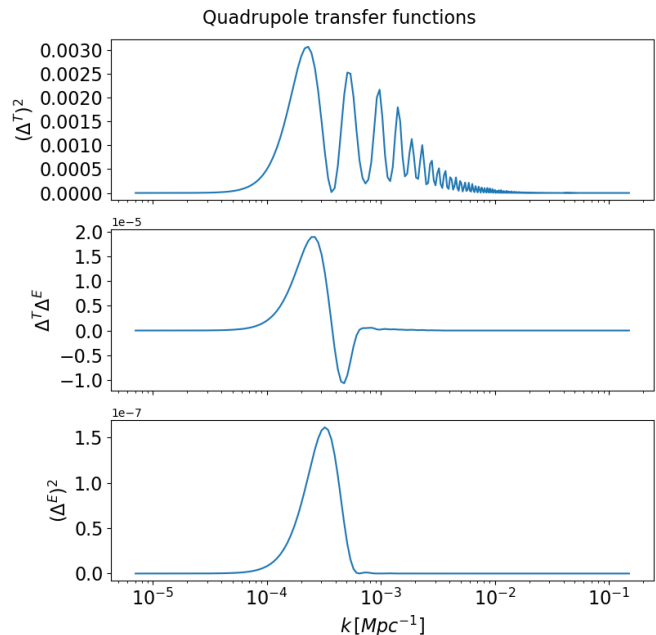


FIG. 2. The CMB quadrupole transfer functions for the temperature (top), temperature-polarization (middle), and polarization (bottom) power spectra.

IV. DISCREPANCY BETWEEN QUADRUPOLES AND Λ CDM

A. Noiseless, full-sky observations

We can estimate the level of discrepancy of the measured moments with the Λ CDM expectation analytically. Our aim here is to assess *how much more* unusual the low temperature quadrupole is, in light of the high polarization quadrupole. To do so, we make the simplifying assumption of noiseless measurements taken over a full-sky map. The complications induced by noise and Planck's 86% (50%) sky coverage in temperature (polarization) [30] will reduce the statistical significances but leave the basic conclusions unaltered. We will assess more precisely the impact of imperfect measurements and $f_{\text{sky}} < 1$ in the next subsection.

If primordial perturbations are Gaussian, then each spherical-harmonic coefficient a_{lm} derived from a full-sky map is a Gaussian random variable with zero mean and variance C_l . The estimators \widehat{C}_l^{TT} and \widehat{C}_l^{EE} for the temperature/polarization moments derived from a noiseless full-map are thus χ^2 -distributed variables with $2l + 1$ degrees of freedom. Given the cross-correlation C_l^{TE} between the temperature and polarization spherical-harmonic coefficients, though, the estimators \widehat{C}_l^{TT} and \widehat{C}_l^{EE} are correlated for any given l . The joint PDF for χ^2 variables correlated in this way can be related to the Wishart distribution [31, 32] and is derived in Appendix A. In our case, the variables can be re-

garded as $X = 5C_2^{TT,\text{observed}}/C_2^{TT,\text{expected}}$ and $Y = 5C_2^{EE,\text{observed}}/C_2^{EE,\text{expected}}$, with $n = 5$. The cross-correlation coefficient is $\rho = C_2^{TE}/[C_2^{TT}C_2^{EE}]^{1/2}$. From Planck Legacy Archive data² used by Figs. 1 and 2 in Ref. [3], we estimate this to be $\rho \simeq 3/\sqrt{(1000) \times (0.055)} \simeq 0.5$. Again, from these data, we infer a measured value of $Y \simeq 18$ (the polarization quadrupole is roughly three times its expected value, $2l + 1 = 5$) and $X \simeq 1.1$, 0.22 times the expected value

First, let's re-visit the temperature quadrupole. The cumulative distribution for a χ^2 -distributed variable X with 5 degrees of freedom below one fifth the mean value is about 4.5%, implying that a departure from the mean of this magnitude will occur (taking into account the possibility of an unusually high fluctuation) in roughly 1 out of every 11 trials, about a 1.7σ fluctuation. The fluctuation in the polarization quadrupole is more significant—roughly a 2.7σ departure, a 1-in-150 occurrence.

If, however, we take into account the joint PDF for the two quadrupoles, the observed values of the two quadrupoles together occur in roughly one in 25,000 realizations, a 4.1σ fluctuation.

B. Imperfect measurements on a cut sky

What we obtain from Planck is not the idealized picture of the microwave sky heretofore discussed. The measured power spectra contain contributions from residual foregrounds and instrumental systematics, and they are made on a masked sky map. Any statements regarding the statistical significance of CMB anomalies must account for these limitations. Here we introduce a simple model to approximate the effects of partial-sky coverage and instrumental noise.

To begin, we recall that for a full-sky map and no noise, the PDF for the observed temperature/polarization quadrupoles are given by $P(X, Y)$ with $X = 5C_2^{TT,\text{obs}}/C_2^{TT,\text{exp}}$ and $Y = 5C_2^{EE,\text{obs}}/C_2^{EE,\text{exp}}$, with $n = 5$ and $\rho = C_2^{TE}/[C_2^{TT}C_2^{EE}]^{1/2}$.

Instrumental noise provides additional contributions

$C_l^{TT,n}$ and $C_l^{EE,n}$ to the temperature and polarization power spectra, respectively, but none to the cross-correlation. In practice, the temperature noise in Planck is negligible for the quadrupole and so we neglect it. With these assumptions (still assuming full-sky coverage), the a_{2m}^T are still distributed with variance C_l^{TT} . The measured a_{2m}^E include both signal and noise and are distributed with variance $C_2^{EE} + C_2^{EE,n}$. The joint PDF for the observed quadrupoles is then $P(X, Y)$ where now $Y = 5(C_2^{EE,\text{obs}} + C_2^{EE,n})/(C_2^{EE} + C_2^{EE,n})$. Note that here, $C_2^{EE,\text{obs}} = C_2^{EE,\text{meas}} - C_2^{EE,n}$; i.e., it is the true quadrupole we infer from the measured quadrupole after subtracting the expected noise contribution. The cross-correlation coefficient is now reduced to $\rho = C_2^{TE}/[C_2^{TT}(C_2^{EE} + C_2^{EE,n})]^{1/2}$.

Now consider the effects of fractional sky coverage. This would be easy if both the temperature and polarization maps had the same f_{sky} . In this case, we would replace $n = 5 \rightarrow 5f_{\text{sky}}$ and also replace $5 \rightarrow 5f_{\text{sky}}$ in the definitions of X and Y . However, given that f_{sky} is different for polarization and temperature, a bit more thought is required. To treat this, we first consider the temperature quadrupole. The PDF for this can simply be taken to be a $\chi_{f_{\text{sky}}^{2(2l+1)}}^2$ distribution. We can then infer from Eq. (A3) the conditional PDF, for our given C_2^{TT} , for C_2^{EE} with n scaled by f_{sky}^E .

To be more precise, we first note that

$$P_n(X) \equiv \int_0^\infty dY P_n(X, Y; \rho), \quad (11)$$

is a χ_n^2 distribution for X . We then note that the conditional probability for Y , given some value X , is

$$P_n(Y; X, \rho) = \frac{P_n(X, Y; \rho)}{P_n(X)}. \quad (12)$$

The unnormalized joint PDF for the temperature quadrupole $C_2^{TT,\text{obs}}$ observed over f_{sky}^T of the sky and polarization quadrupole $C_2^{EE,\text{obs}}$ observed over f_{sky}^E of the sky shown in Fig. 3 is

$$\frac{P_{5f_{\text{sky}}^T} \left(5f_{\text{sky}}^T C_2^{TT,\text{obs}}/C_2^{TT,\text{exp}} \right)}{P_{5f_{\text{sky}}^E} \left(5f_{\text{sky}}^E C_2^{TT,\text{obs}}/C_2^{TT,\text{exp}} \right)} P_{5f_{\text{sky}}^E} \left(5f_{\text{sky}}^E \frac{C_2^{TT,\text{obs}}}{C_2^{TT,\text{exp}}}, 5f_{\text{sky}}^E \frac{C_2^{EE,\text{obs}} + C_2^{EE,n}}{C_2^{EE,\text{exp}} + C_2^{EE,n}}; \rho \right). \quad (13)$$

The two-tailed probability of getting a temperature quadrupole at least as extreme as we observe, given Planck's limited sky coverage, is 12.8% or a 1.5σ fluctua-

tion. Table 3 of Ref. [30] gives the probability of obtaining a polarization quadrupole as anomalous as measured as 29.6%, or 1σ , based on FFP10 simulations [33]. From this result, we can solve for Y using the equation

$$\int_Y^\infty \chi^2(5f_{\text{sky}}^E, Y) dY = 0.296/2 \quad (14)$$

² <http://pla.esac.esa.int/pla/#home>

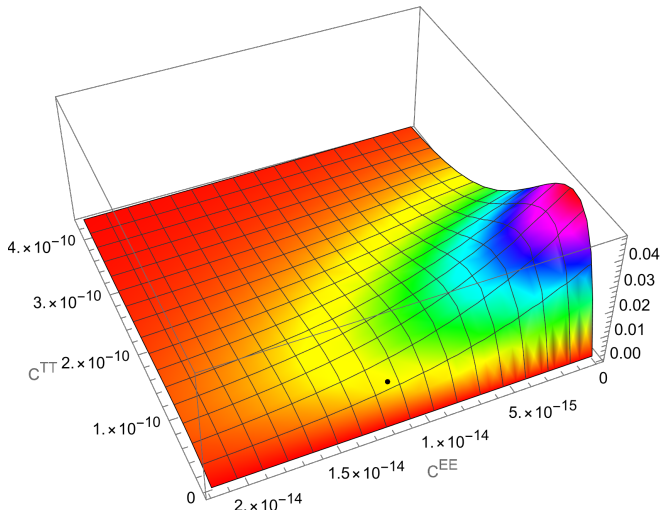


FIG. 3. The unnormalized PDF of Eq. (13), ranging from lower values in red to higher values in purple. The black point corresponds to the observed temperature and polarization quadrupole values.

which gives $Y = 4.6$. The amount of noise is thus $C_2^{EE,n} = 4.1 \times 10^{-15}$. We now have all the ingredients required to calculate the joint probability. Integrating Eq. (13) and dividing by its normalization factor gives a two-tailed probability of 2.1% or 2.3σ .

V. A LARGE-SCALE MODIFICATION TO Λ CDM

Taken at face value, the results of Section IV are in minor conflict with the standard-cosmological-model expectations. We thus consider a modification to Λ CDM in which we modify the matter power spectrum $P_m(k)$ at $k \lesssim 10^{-3} \text{ Mpc}^{-1}$. This appears in the low- l CMB power spectra but not in large-scale structure surveys which probe higher k . For simplicity, we do not consider any effects that modifying the power spectrum will have on the inferred cosmological parameters.

The full CMB quadrupole transfer functions are shown in Fig. 2. From here we can see that even though temperature and E-mode polarization probe different epochs, the two extend over comparable distance scales. This provides us a k range over which to invoke new physics and subsequently alter the matter power spectrum.

We first consider decreasing $P_m(k)$ by $P_m \rightarrow P_m/17$ for $k < 3 \times 10^{-4} \text{ Mpc}^{-1}$. This is one way ensure that our modified Λ CDM model correctly predicts $C_2^{TT,obs}$. The complete set of model predictions are $C_2^{TT} = 3.18 \times 10^{-11}$, $C_2^{TE} = 5.52 \times 10^{-14}$, and $C_2^{EE} = 3.17 \times 10^{-16}$; this implies that the probability of our model generating an E-mode quadrupole at least as discrepant as $C_2^{EE,obs}$ is 4.1%. Put another way, observations and the-

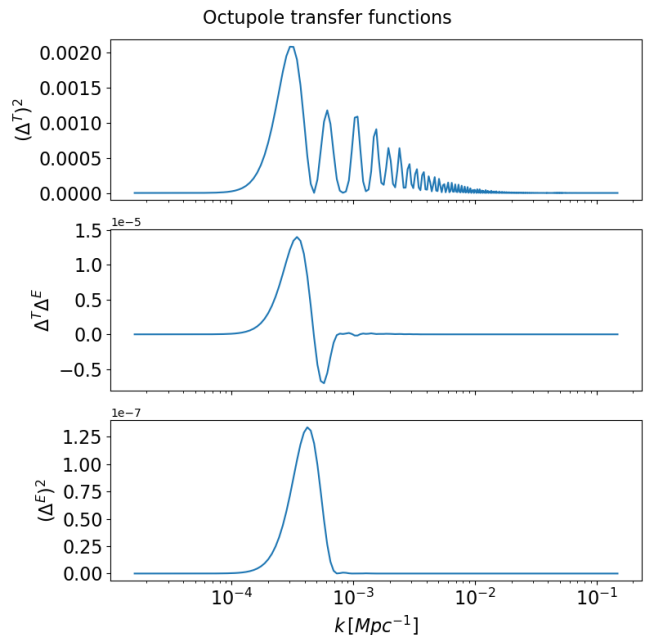


FIG. 4. Same as Fig 2 but for the octupole moment.

ory would be in tension at 2σ . If instead we appropriately boost the large-scale power of our model to agree with $C_2^{EE,obs}$, the probability of having an anomalous temperature quadrupole comparable to or greater than what we see is 2.6% or a 2.2σ discrepancy. We conclude that the tension between the two quadrupoles is not easily resolved by an increase/decrease of large-scale power.

VI. CONCLUSIONS

The low CMB temperature quadrupole has been a curiosity for three decades [1]. Although the inconsistency with its expected value is not that statistically significant, the fact that the power on the *largest* observable scale is low has been interpreted as a possible hint of new super-horizon physics. The independent confirmation of a low quadrupole by WMAP [2] and then Planck [3] suggests that this low quadrupole is robust.

More recently, however, Planck has found the CMB polarization quadrupole to be somewhat high. Here we have calculated the joint PDF for the two quadrupoles and found that they are inconsistent with the Λ CDM expectation at the 2.3σ level. We also argued that the inconsistency is robust to simple changes to the cosmological model.

What to make of this result? It is obvious to wonder whether the Planck polarization result may be skewed high by some instrumental systematic and/or unusual foreground contamination. The former was mitigated a few years ago with the development of the SR0112 algorithm [34], while the latter was considered more recently with the updated SR0113 neural network [35]. Re-

sults using the **SRo112** algorithm included a lower measured value for C_2^{EE} with a PTE of 38%, while the PTE for C_2^{TE} decreased to 58.1% [36]. The temperature-polarization joint probability was not calculated, but we expect it to be similar to the PR3 results calculated in this work.

Fortunately, though, COBE, WMAP, and Planck will not be our only sources of quadrupole-scale CMB measurements for long. The forthcoming LiteBIRD experiment will target precise polarization measurements on the largest angular scales, with unprecedented frequency coverage to enable foreground removal over the entire sky. The anomaly should also motivate the search for some type of calibration of the polarization quadrupole, analogous to that suggested for the temperature quadrupole in Ref. [37] (the peculiar-velocity-induced temperature quadrupole discussed in there does not produce a polarization quadrupole). If the marginally high polarization quadrupole persists, it will then disfavor explanations for the low quadrupole that involved suppressed large-scale power. But will it then simply be chalked up to a statistical fluctuation? Or perhaps some other new physics?

ACKNOWLEDGEMENTS

We thank J. Dunkley for useful discussions. This work was supported at Johns Hopkins by NSF Grant No. 2112699 and the Simons Foundation. JG acknowledges support from Princeton's Presidential Postdoctoral Research Fellowship.

Appendix A: Derivation of the joint χ^2 probability distribution function

Let x and y be Gaussian random variables with unit variance, zero mean, and covariance $\langle xy \rangle = \rho$. If we have n realizations x_i and y_i (for $i = 1, \dots, n$) of these pairs, then the joint probability distribution function (PDF) for these $2n$ random variables is

$$p(\vec{x}, \vec{y}) = \frac{1}{(2\pi)^n (1 - \rho^2)^{n/2}} \exp \left[-\frac{\vec{x}^2 + \vec{y}^2 - 2\rho \vec{x} \cdot \vec{y}}{2(1 - \rho^2)} \right], \quad (\text{A1})$$

where \vec{x} and \vec{y} are n -dimensional vectors with components x_i and y_i , respectively.

We now define two variables $X \equiv \vec{x}^2$ and $Y \equiv \vec{y}^2$ which are correlated χ^2 variables with joint PDF,

$$P_n(X, Y; \rho) = \int d^n x \int d^n y p(\vec{x}, \vec{y}) \delta_D(X - \vec{x}^2) \delta_D(Y - \vec{y}^2), \quad (\text{A2})$$

where $\delta_D(x)$ is the Dirac delta function. The probability distribution is a function of the vector norms \vec{x}^2 and \vec{y}^2 , and also the dot product $\vec{x} \cdot \vec{y}$, and we are integrating over all \vec{x} and all \vec{y} . The integration over \vec{x} can be written as $S_{n-1} \int x^{n-1} dx$, where $S_{n-1} = 2\pi^{n/2}/\Gamma(n/2)$ is the volume of the unit n -sphere. The integration over \vec{y} can then be written as $S_{n-2} \int dy_1 \int y_\perp^{n-2} dy_\perp$, where y_1 is the component of \vec{y} along the direction of \vec{x} and $\vec{y}_\perp = (y_2, \dots, y_n)$ the components perpendicular to \vec{x} . We then write $x^{n-1} dx = (x^2)^{(n/2)-1} d(x^2)/2$, $y_\perp^{n-2} dy_\perp = (y_\perp^2)^{(n/2)-(3/2)} d(y_\perp^2)/2$, and the argument of the second Dirac delta function in Eq. (A2) as $(Y - y_1^2) - y_\perp^2$. We then find

$$P_n(X, Y; \rho) = \frac{(XY)^{\frac{n}{2}-1}}{2^n (1 - \rho^2)^{n/2} [\Gamma(n/2)]^2} \exp \left[-\frac{X + Y}{2(1 - \rho^2)} \right] \times G_n \left(\frac{\rho \sqrt{XY}}{1 - \rho^2} \right), \quad (\text{A3})$$

where

$$G_n(\alpha) \equiv \frac{1}{\sqrt{\pi}} \frac{\Gamma(\frac{n}{2})}{\Gamma(\frac{n-1}{2})} \int_{-1}^1 d\mu (1 - \mu^2)^{\frac{n}{2}-\frac{3}{2}} e^{\alpha\mu}. \quad (\text{A4})$$

Mathematica can write the integral in terms of a hypergeometric function, which provides little insight but may facilitate numerical evaluation.

-
- [1] C. L. Bennett, A. Banday, K. M. Gorski, G. Hinshaw, P. Jackson, P. Keegstra, A. Kogut, G. F. Smoot, D. T. Wilkinson, and E. L. Wright, Four year COBE DMR cosmic microwave background observations: Maps and basic results, *Astrophys. J. Lett.* **464**, L1 (1996), arXiv:astro-ph/9601067.
- [2] C. L. Bennett et al. (WMAP), Nine-Year Wilkinson Microwave Anisotropy Probe (WMAP) Observations: Final Maps and Results, *Astrophys. J. Suppl.* **208**, 20 (2013), arXiv:1212.5225 [astro-ph.CO].
- [3] N. Aghanim et al. (Planck), Planck 2018 results. VI. Cosmological parameters, *Astron. Astrophys.* **641**, A6 (2020), [Erratum: *Astron. Astrophys.* 652, C4 (2021)], arXiv:1807.06209 [astro-ph.CO].
- [4] D. Boyanovsky, H. J. de Vega, and N. G. Sanchez, CMB quadrupole suppression. 1. Initial conditions of inflationary perturbations, *Phys. Rev. D* **74**, 123006 (2006), arXiv:astro-ph/0607508.
- [5] X. Chen, R. Easter, and E. A. Lim, Generation and Characterization of Large Non-Gaussianities in Single

- Field Inflation, *JCAP* **04**, 010, arXiv:0801.3295 [astro-ph].
- [6] E. Ramirez and D. J. Schwarz, Predictions of just-enough inflation, *Phys. Rev. D* **85**, 103516 (2012), arXiv:1111.7131 [astro-ph.CO].
- [7] E. Dudas, N. Kitazawa, S. P. Patil, and A. Sagnotti, CMB Imprints of a Pre-Inflationary Climbing Phase, *JCAP* **05**, 012, arXiv:1202.6630 [hep-th].
- [8] C. R. Contaldi, M. Peloso, L. Kofman, and A. D. Linde, Suppressing the lower multipoles in the CMB anisotropies, *JCAP* **07**, 002, arXiv:astro-ph/0303636.
- [9] C. Destri, H. J. de Vega, and N. G. Sanchez, The pre-inflationary and inflationary fast-roll eras and their signatures in the low CMB multipoles, *Phys. Rev. D* **81**, 063520 (2010), arXiv:0912.2994 [astro-ph.CO].
- [10] M. Cicoli, S. Downes, B. Dutta, F. G. Pedro, and A. Westphal, Just enough inflation: power spectrum modifications at large scales, *JCAP* **2014** (12), 030, arXiv:1407.1048 [hep-th].
- [11] N. Kitazawa and A. Sagnotti, A string-inspired model for the low- ℓ CMB, *Mod. Phys. Lett. A* **30**, 1550137 (2015), arXiv:1503.04483 [hep-th].
- [12] R. Bousso, D. Harlow, and L. Senatore, Inflation after False Vacuum Decay: observational Prospects after Planck, *Phys. Rev. D* **91**, 083527 (2015), arXiv:1309.4060 [hep-th].
- [13] J. Chluba, J. Hamann, and S. P. Patil, Features and New Physical Scales in Primordial Observables: Theory and Observation, *Int. J. Mod. Phys. D* **24**, 1530023 (2015), arXiv:1505.01834 [astro-ph.CO].
- [14] Y. Akrami et al. (COMPACT), The Search for the Topology of the Universe Has Just Begun, (2022), arXiv:2210.11426 [astro-ph.CO].
- [15] M. Braglia, D. K. Hazra, L. Sriramkumar, and F. Finelli, Generating primordial features at large scales in two field models of inflation, *JCAP* **08**, 025, arXiv:2004.00672 [astro-ph.CO].
- [16] H. V. Ragavendra, D. Chowdhury, and L. Sriramkumar, Suppression of scalar power on large scales and associated bispectra, *Phys. Rev. D* **106**, 043535 (2022), arXiv:2003.01099 [astro-ph.CO].
- [17] D. N. Spergel et al. (WMAP), First year Wilkinson Microwave Anisotropy Probe (WMAP) observations: Determination of cosmological parameters, *Astrophys. J. Suppl.* **148**, 175 (2003), arXiv:astro-ph/0302209.
- [18] C. J. Copi, D. Huterer, D. J. Schwarz, and G. D. Starkman, No large-angle correlations on the non-Galactic microwave sky, *Mon. Not. Roy. Astron. Soc.* **399**, 295 (2009), arXiv:0808.3767 [astro-ph].
- [19] C. J. Copi, D. Huterer, D. J. Schwarz, and G. D. Starkman, Large angle anomalies in the CMB, *Adv. Astron.* **2010**, 847541 (2010), arXiv:1004.5602 [astro-ph.CO].
- [20] Y. Akrami et al. (Planck), Planck 2018 results. VII. Isotropy and Statistics of the CMB, *Astron. Astrophys.* **641**, A7 (2020), arXiv:1906.02552 [astro-ph.CO].
- [21] A. Yoho, C. J. Copi, G. D. Starkman, and A. Kosowsky, Probing Large-Angle Correlations with the Microwave Background Temperature and Lensing Cross Correlation, *Mon. Not. Roy. Astron. Soc.* **442**, 2392 (2014), arXiv:1310.7603 [astro-ph.CO].
- [22] C. J. Copi, D. Huterer, D. J. Schwarz, and G. D. Starkman, Large-Angle CMB Suppression and Polarization Predictions, *Mon. Not. Roy. Astron. Soc.* **434**, 3590 (2013), arXiv:1303.4786 [astro-ph.CO].
- [23] A. Yoho, S. Aiola, C. J. Copi, A. Kosowsky, and G. D. Starkman, Microwave Background Polarization as a Probe of Large-Angle Correlations, *Phys. Rev. D* **91**, 123504 (2015), arXiv:1503.05928 [astro-ph.CO].
- [24] Y. Akrami et al., Planck 2018 results. X. Constraints on inflation, *Astron. Astrophys.* **641**, A10 (2020), arXiv:1807.06211 [astro-ph.CO].
- [25] E. Allys et al. (LiteBIRD), Probing Cosmic Inflation with the LiteBIRD Cosmic Microwave Background Polarization Survey, *PTEP* **2023**, 042F01 (2023), arXiv:2202.02773 [astro-ph.IM].
- [26] J. Jones, C. J. Copi, G. D. Starkman, and Y. Akrami, The Universe is not statistically isotropic, arXiv e-prints, arXiv:2310.12859 (2023), arXiv:2310.12859 [astro-ph.CO].
- [27] J. Lesgourgues, The Cosmic Linear Anisotropy Solving System (CLASS) I: Overview, (2011), arXiv:1104.2932 [astro-ph.IM].
- [28] A. Lewis, A. Challinor, and A. Lasenby, Efficient computation of CMB anisotropies in closed FRW models, *Astrophys. J.* **538**, 473 (2000), arXiv:astro-ph/9911177.
- [29] L. Ji, S. C. Hotinli, and M. Kamionkowski, Cross-correlation of the polarizations of the 21-cm and cosmic microwave backgrounds, *Phys. Rev. D* **107**, 123533 (2023), arXiv:2110.01619 [astro-ph.CO].
- [30] N. Aghanim et al., Planck 2018 results. V. CMB power spectra and likelihoods, *Astron. Astrophys.* **641**, A5 (2020), arXiv:1907.12875 [astro-ph.CO].
- [31] W. J. Percival and M. L. Brown, Likelihood techniques for the combined analysis of CMB temperature and polarization power spectra, *Mon. Not. R. Astron. Soc.* **372**, 1104 (2006), arXiv:astro-ph/0604547 [astro-ph].
- [32] S. Hamimeche and A. Lewis, Likelihood analysis of CMB temperature and polarization power spectra, *Phys. Rev. D* **77**, 103013 (2008), arXiv:0801.0554 [astro-ph].
- [33] Planck Collaboration, N. Aghanim, et al., Planck 2018 results. III. High Frequency Instrument data processing and frequency maps, *Astron. & Astrophys.* **641**, A3 (2020), arXiv:1807.06207 [astro-ph.CO].
- [34] J. M. Delouis, L. Pagano, S. Mottet, J. L. Puget, and L. Vibert, SRoll2: an improved mapmaking approach to reduce large-scale systematic effects in the Planck High Frequency Instrument legacy maps, *Astron. & Astrophys.* **629**, A38 (2019), arXiv:1901.11386 [astro-ph.CO].
- [35] M. Lopez-Radcenca, J. M. Delouis, and L. Vibert, SRoll3: A neural network approach to reduce large-scale systematic effects in the Planck High-Frequency Instrument maps, *Astron. & Astrophys.* **651**, A65 (2021), arXiv:2012.09702 [astro-ph.IM].
- [36] L. Pagano, J. M. Delouis, S. Mottet, J. L. Puget, and L. Vibert, Reionization optical depth determination from Planck HFI data with ten percent accuracy, *Astron. & Astrophys.* **635**, A99 (2020), arXiv:1908.09856 [astro-ph.CO].
- [37] M. Kamionkowski and L. Knox, Aspects of the cosmic microwave background dipole, *Phys. Rev. D* **67**, 063001 (2003), arXiv:astro-ph/0210165 [astro-ph].